The Affinity of Magnesium Binding Sites in the *Bacillus subtilis* RNase P·Pre-tRNA Complex Is Enhanced by the Protein Subunit†

Jeffrey C. Kurz‡ and Carol A. Fierke*

Department of Chemistry, University of Michigan, 930 North University, Ann Arbor, Michigan 48109-1055

Received January 15, 2002; Revised Manuscript Received May 1, 2002

ABSTRACT: The RNA subunit of bacterial ribonuclease P (RNase P) requires high concentrations of magnesium ions for efficient catalysis of tRNA 5′-maturation in vitro. The protein component of RNase P, required for cleavage of precursor tRNA in vivo, enhances pre-tRNA binding by directly contacting the 5′-leader sequence. Using a combination of transient kinetics and equilibrium binding measurements, we now demonstrate that the protein component of RNase P also facilitates catalysis by specifically increasing the affinities of magnesium ions bound to the RNase P·pre-tRNA^{Asp} complex. The protein component does not alter the number or apparent affinity of magnesium ions that are either diffusely associated with the RNase P RNA polyanion or required for binding mature tRNA^{Asp}. Nor does the protein component alter the pH dependence of pre-tRNA^{Asp} cleavage catalyzed by RNase P, providing further evidence that the protein component does not directly stabilize the catalytic transition state. However, the protein subunit does increase the affinities of at least four magnesium sites that stabilize pre-tRNA binding and, possibly, catalysis. Furthermore, this stabilizing effect is coupled to the P protein/5′-leader contact in the RNase P holoenzyme·pre-tRNA complex. These results suggest that the protein component enhances the magnesium affinity of the RNase P·pre-tRNA complex *indirectly* by binding and positioning pre-tRNA. Furthermore, RNase P is inhibited by cobalt hexammine ($K_I = 0.11 \pm 0.01$ mM) while magnesium, manganese, cobalt, and zinc compete with cobalt hexammine to activate RNase P. These data are consistent with the hypothesis that catalysis by RNase P requires at least one metal−water ligand or one inner-sphere metal contact.

Ribonuclease P (RNase P)[1] catalyzes the essential 5′-maturation of precursor tRNA (pre-tRNA) in all organisms by the cleavage of a specific phosphodiester bond, yielding 5′-phosphate and 3′-hydroxyl end groups (*1*−*3*). Bacterial RNase P consists of a single RNA subunit of ∼400 nucleotides and a single protein subunit of ∼120 amino acids, and both subunits are required for pre-tRNA processing in vivo (*4*−*7*). The RNA component alone (P RNA) is sufficient for catalysis of pre-tRNA cleavage in vitro (*8*); hence, P RNA is a ribozyme. However, compared to the holoenzyme-catalyzed reaction, the P RNA-catalyzed reaction requires high concentrations of monovalent and divalent cations (*8*−*10*). In the cell, the total concentration of magnesium ion has been estimated as 30 mM, but the free concentration of magnesium is ∼1 mM (*11, 12*). Therefore, one role of the protein component (P protein) is to decrease the magnesium ion requirement of RNase P.

Magnesium ions fulfill multiple functional roles in RNase P. Direct measurement of the interaction between magnesium and P RNA (*13*) demonstrates that >100 magnesium ions associate nonspecifically with P RNA, by electrostatic forces, to screen repulsive interactions between phosphates of the P RNA backbone and to promote formation of a compact tertiary structure (*14*). Several additional magnesium ions are proposed to bind to specific sites to promote P RNA folding (*15, 16*) and stabilize ground and transition state interactions with the pre-tRNA substrate (*13, 17*). The protein component could promote catalysis at physiological magnesium concentrations by increasing the stability of Mg^{2+}/P RNA interactions in one or more of these roles, or by promoting the formation of additional magnesium ion binding sites.

Functional studies indicate that the protein component of *B. subtilis* RNase P has modest effects on the global folding of P RNA, as measured by Fe(II)-induced hydroxyl-radical cleavage (*16*). Therefore, the effect of the protein component on the magnesium ion dependence of catalysis is not mediated through stabilization of the global tertiary structure of P RNA, as observed for other protein−RNA complexes (*18, 19*). In fact, kinetic and thermodynamic studies demonstrate that the protein subunit enhances the affinity of *B.*

† Supported by National Institutes of Health Grant GM 55387. J.C.K. was supported in part by NIH Training Grant GM 08487.

* To whom correspondence should be addressed. Tel: (734)-936-2678, FAX: (734)-647-4865, E-mail: fierke@umich.edu.

‡ Current address: Archemix Corp., One Hampshire St., Cambridge, MA 02139.

[1] Abbreviations: 5′P, 5′ precursor tRNA fragment; Amp, 2-amino-2-methyl-1-propanol; CH_3COOH/Mes/Tris buffer, 25 mM acetic acid, 25 mM Mes, 50 mM Tris; E, RNase P RNA or RNase P holoenzyme; EDTA, (ethylenedinitrilo)tetraacetic acid; HQS, 8-hydroxyquinoline-5-sulfonic acid; Mes, 2-(*N*-morpholino)ethanesulfonic acid; Mes/Tris buffer, 50 mM Mes, 50 mM Tris; Mes/Tris/Amp buffer, 50 mM Mes, 25 mM Tris, 25 mM Amp; PEI, polyethylenimine; pre-tRNA, precursor to transfer RNA; RNase P, ribonuclease P; RNase P RNA or P RNA, RNA component of RNase P; RNase P protein or P protein, protein component of RNase P; S or pre-tRNA^{Asp}, precursor tRNA^{Asp}; SDS, sodium dodecyl sulfate; Tris, tris(hydroxymethyl)aminomethane; UpG, uridylyl (3′→5′)-guanosine.

10.1021/bi025553w CCC: $22.00
Published on Web 07/04/2002

subtilis RNase P for pre-tRNA^{Asp} by 10^4-fold, without substantially affecting the cleavage rate constant or mature tRNA binding (*20, 21*). Moreover, cross-linking experiments using photoagent-modified P proteins (*22*) indicate that this enhancement depends on direct contacts between the 5′-leader sequence of pre-tRNA and amino acids in the P protein "central cleft" (*23*).

Here we examine the effects of the P protein on both specific and nonspecific magnesium ion interactions in *B. subtilis* RNase P. The protein subunit exerts little effect on the nonspecific, electrostatic association of RNase P with bulk magnesium ions or the specific magnesium ions that mediate the binding of the mature tRNA^{Asp} product. However, measurements of the magnesium ion dependence of the cleavage rate constant indicate that the protein subunit increases the affinity of the RNase P·pre-tRNA complex for specific magnesium ions. Therefore, we envision that favorable contacts between the protein and the 5′-leader sequence stabilize (either directly or indirectly) specific magnesium sites formed in the P RNA·pre-tRNA binary complex.

Furthermore, the effects of the protein component on the potential catalytic roles of magnesium ions are also addressed. The pH dependence of the pre-tRNA cleavage rate constant catalyzed by the RNase P holoenzyme indicates that the protein subunit does not alter the observed pK_a for catalysis. This ionization has been proposed to reflect a role for hydroxide as a general base or nucleophile in the catalytic mechanism (*17*), possibly stabilized by coordination to a magnesium ion (*24, 25*). Competition between magnesium and the inert $Mg(H_2O)_6^{2+}$ analogue cobalt(III) hexammine $[Co(NH_3)_6^{3+}]$ (*26*) suggests that pre-tRNA cleavage depends on at least one bound magnesium ion. Furthermore, this magnesium ion can be functionally substituted by other transition metals, including manganese(II) and zinc(II).

In summary, these data demonstrate that a main function of the protein component in bacterial RNase P is to interact with the 5′ leader sequence which enhances the affinity of both pre-tRNA and specific magnesium ions bound to the RNase P·pre-tRNA complex.

MATERIALS AND METHODS

RNA and Protein Preparation. B. subtilis P RNA and variants of *B. subtilis* pre-tRNA^{Asp} containing leader sequences of varying lengths (*20*) were prepared by in vitro transcription from linearized plasmids with T7 RNA polymerase (*27*). Mature tRNA^{Asp} and substrates with leader sequences of two nucleotides (GU-) and longer were transcribed in the presence of 1 mM each of ATP, CTP, UTP, and GTP and 4 mM guanosine to produce RNA containing a 5′-hydroxyl group (*20*). A substrate with one uracil on the 5′ side of the cleavage site (1-tRNA) was prepared by including 4 mM UpG (Sigma) in the transcription reaction in place of guanosine (*20*). Substrate RNAs were labeled at the 5′-end by incubation with [γ-^{32}P]ATP and T4 polynucleotide kinase (New England Biolabs), and purified by denaturing (7 M urea) 8% polyacrylamide gel electrophoresis (PAGE), as described (*21*). Substrate RNAs were further purified by ethanol precipitation followed by gel filtration over a G-25 Sephadex centrifuge column. Centrifuge columns (0.5 mL bed volume) were prepared in Spin-X centrifuge filters (0.22 μM cellulose acetate membrane; Costar) and equilibrated with 10 mM Tris-HCl, pH 8.0. Large quantities of P RNA (30−40 mg) were purified by denaturing 5% PAGE, and eluted into TE buffer (10 mM Tris-HCl, pH 8, 1 mM EDTA) containing 0.1% sodium dodecyl sulfate, as described (*28*). Eluted P RNA was concentrated by ethanol precipitation, and 5 mg portions were further purified using "RNeasy" columns (Qiagen) or PD-10 gel filtration columns (Amersham-Pharmacia) equilibrated in 10 mM Tris-HCl, pH 8.0, to remove residual urea and SDS. The RNA was again precipitated with ethanol and resuspended in 10 mM Tris-HCl, pH 8.0, to prepare a concentrated stock (>0.1 mM). Concentrations of RNAs were determined by measuring the absorbance at 260 nm as previously described (*28*). RNAs were refolded by incubation at 95 °C for 3 min, followed by a 2-fold dilution into 2× reaction buffer and incubation at 37 °C for 15 min.

The recombinant protein component of *B. subtilis* RNase P was expressed in BL21(DE3)pLysS *E. coli* (*29*) containing the plasmid pPWT-1 by growth at 37 °C followed by induction with isopropylthio-β-D-galactopyranoside, as described (*30*). The protein was purified by chromatography over CM-Sepharose, and the concentration was determined by measuring the absorbance at 280 nm (ϵ_{280} = 6000 M^{-1} cm^{-1}; *30*). Holoenzyme was reconstituted immediately prior to use by incubation of refolded P RNA with a slight excess concentration of protein at 37 °C for 10 min.

A tRNA^{Asp} precursor containing a specific 2′-deoxy modification at the cleavage site was prepared according to the RNA ligation method of Moore and Sharp (*31*). RNA ligations were performed using histidine-tagged T4 DNA ligase, purified from an overexpressing strain provided by Prof. Scott Strobel; 5 nmol of mature tRNA^{Asp} (containing a 5′-phosphate group) and 2.5 nmol of a 13-nucleotide DNA/RNA hybrid oligonucleotide (5′-GUA-CCC-AAA-ACA-dU-3′; Oligos Etc.) were annealed to 2.5 nmol of a 27 nucleotide DNA "splint" (5′-dTGA-ACT-ACC-GGA-CCA-TGT-TTT-GGG-TAC-A) complementary to both the oligonucleotide sequence and a 14-nucleotide sequence at the 5′ end of mature tRNA^{Asp}, in 100 μL of TE buffer (10 mM Tris, 1 mM EDTA, pH 8.0) containing 50 mM NaCl by heating the mixture to 95 °C for 10 min followed by slowly cooling (∼1 h) to room temperature. This reaction was then diluted into 2.5 mL of 66 mM Tris-HCl, pH 7.5, 6.6 mM $MgCl_2$, 10 mM dithiothreitol, 66 μM ATP, 30% glycerol, and 3 nmol of T4 DNA ligase, and incubated for 6 h at 25 °C. The ligated product was separated from the reactants by gel electrophoresis (10% polyacrylamide), and approximately 0.8 nmol (∼30% yield) of pre-tRNA was recovered.

Single-Turnover Experiments. Experiments measuring single-turnover reactions were carried out using excess enzyme concentrations ([E]/[S] ≥ 5; [E] = 2 nM−20 μM; [S] = 0.2−10 nM) either manually ($t_{1/2}$ ≥ 2 s) or with a model RQF-3 quench-flow apparatus from KinTek Instruments ($t_{1/2}$ ≤ 4 s) at 37 °C as described (*28*). Single-turnover reactions were quenched by dilution into 1 volume of 200 mM EDTA (pH 8.0). For substrates with 5′-leader sequences ≤5 nucleotides in length, the labeled 5′-leader sequence product was separated from pre-tRNA^{Asp} on polyethylenimine−cellulose thin-layer chromatography plates (EM-Science) developed in 1 M LiCl (*20*), while cleavage of longer substrates was analyzed by 8−12% PAGE (*28*). A rate constant measured using the quench-flow (2 μM

holoenzyme, 10 mM $MgCl_2$, 100 mM KCl, pH 6, 37 °C; $k_{obs} = 0.17\ s^{-1}$) was identical to that measured manually under the same conditions (data not shown). The endpoints for these reactions were always 0.8−0.9, indicating that the majority of the substrate was correctly folded.

For studies of the pH dependence of the catalytic rate constant (k_2), the pH was varied using a series of buffer mixtures of constant ionic strength (*32*): CH_3COOH/Mes/Tris buffer (pH 4.7−6.0), 25 mM acetic acid (Aldrich, 99.99+%), 25 mM Mes (SigmaUltra), 50 mM Tris (Aldrich, ultrapure); Mes/Tris buffer (pH 5.0−8.4), 50 mM Mes, 50 mM Tris; or Mes/Tris/Amp buffer (pH 6.0−9.7), 50 mM Mes, 25 mM Tris, 25 mM 2-amino-2-methyl-1-propanol (SigmaUltra). The pH of the buffers was adjusted using HCl (Aldrich, 99.999%) or KOH (SigmaUltra). The studies investigating the magnesium ion dependence of the reaction were mainly carried out in Mes/Tris buffer at pH 5.2 or 6.0. In these reactions, the concentrations of magnesium chloride and potassium chloride (SigmaUltra) were inversely varied to maintain a constant ionic strength.

Mature tRNA Binding. The magnesium ion dependence of mature $tRNA^{Asp}$ binding to RNase P RNA and holoenzyme was measured by incubating 5′-end-labeled $tRNA^{Asp}$ (0.1−1 nM) with a ≥5-fold molar excess of RNase P RNA or holoenzyme (0.002−20 μM) in Mes/Tris buffer (pH 6.0) and varying concentrations of $MgCl_2$ at low (10−35 mM $MgCl_2$, 100−25 mM KCl) or intermediate monovalent ion concentrations (10−90 mM $MgCl_2$, 400−160 mM KCl). Bound and free $tRNA^{Asp}$ were separated by gel filtration over a G-75 Sephadex spin column (*21*). The fraction of $tRNA^{Asp}$ bound was determined as the fraction of total radioactivity found in the eluate, as quantified by Cerenkov scintillation counting (*28*).

Fluorescence Detection Assay for Magnesium Ion. The binding affinities of magnesium ions for RNase P RNA and holoenzyme were measured using the fluorophore 8-hydroxyquinoline-5-sulfonic acid (HQS), as described (*13*); 110 μL samples of RNase P RNA or holoenzyme (3 or 10 μM) were prepared in Mes/Tris/Amp buffer, pH 8.0, containing 0.05−12 mM $MgCl_2$, and 0 or 100 mM KCl, and incubated at 25 °C. Free magnesium ions (Mg_{free}) were separated from magnesium ions bound to RNase P by "forced-dialysis" (*33*) using Microcon-30 centrifugal filter devices (Millipore). Microcon-30 membranes were washed twice with 0.5 mL of metal-free water and once with 1× buffer (no magnesium) to remove glycerin, which interferes with subsequent fluorescence measurements, just prior to loading RNase P into the sample reservoir. The Microcon devices retain a significant, 10 μL "hold-up" volume (unrecoverable volume trapped beneath the membrane); therefore, samples were immediately centrifuged for ∼1.5 min at 10 000 rpm to elute ∼50 μL of solution. This eluate was added back to the sample reservoir, and the sample was incubated in the Microcon device for an additional 15−20 min at 25 °C to allow the magnesium ion concentration to equilibrate. The samples were then centrifuged for 35−40 s at 5000 rpm to elute 10−15 μL. To quantify the concentration of magnesium in the retentate ($[Mg^{2+}]_{total}$), and in the eluate ($[Mg^{2+}]_{free}$), 10 μL of each was diluted into 150 μL of 2 mM HQS, 5 M guanidine hydrochloride, and 0.1 M Tris−SO_4, pH 8.0 (*13*). The fluorescence of these samples was measured in a 120 μL fluorescence cell at 25 °C using an Aminco-Bowman Series 2 luminescence spectrometer (excitation = 397 nm; emission = 502 nm). The magnesium ion concentration of the sample was determined by comparison of the fluorescence to a standard curve using known concentrations of $MgCl_2$ (linear from 0 to 20 μM) (*13*).

Data Analysis. Single-turnover data were analyzed using Kaleidagraph (Synergy Software). For substrates containing leader sequences of two nucleotides and longer, single-turnover holoenzyme data were analyzed assuming a mechanism of two consecutive irreversible first-order reactions (eq 1), since substrate dissociation is slower than cleavage, as indicated by the presence of lags in the timecourses at intermediate concentrations of holoenzyme (*34*).

$$[P]_t = [\text{pre-tRNA}]_0\left[1 + \frac{1}{k_1[E] - k_2}(k_2 e^{-k_1[E]t} - k_1[E]e^{-k_2 t})\right] \quad (1)$$

$$[P]_t = [P]_\infty \times (1 - e^{-k_2 t}) \quad (2)$$

Holoenzyme-catalyzed cleavage of 1-tRNA at pH 5.2 (10−50 mM $MgCl_2$) and pH 6.0 (5−20 mM $MgCl_2$) was well described by a single-exponential (eq 2) at all holoenzyme concentrations. Therefore, the dependence of k_{obs} on [E] was analyzed assuming a rapid equilibrium mechanism ($k_{-1} \gg k_2$), using eq 3, where K_D is the dissociation constant for 1-tRNA, and $k_{1,app}$ is the apparent second-order rate constant ($=k_2/K_D$ for this mechanism).

$$k_{obs} = k_2[E]/(K_D + [E]) = k_{1,app}[E]/(1 + [E]/K_D) \quad (3)$$

Where indicated, the magnesium ion dependencies of single-turnover rate constants were analyzed by the Hill equation (*35*):

$$k_{obs} = k_{max}([Mg^{2+}]^{\alpha_H}/{K_{1/2}}^{\alpha_H})/(1 + [Mg^{2+}]^{\alpha_H}/{K_{1/2}}^{\alpha_H}) \quad (4)$$

where k_{obs} is the rate constant at a specific magnesium ion concentration, k_{max} is the rate constant at saturating magnesium, $K_{1/2}$ is the magnesium ion concentration at which $k_{obs} = 1/2 \times k_{max}$, and α_H is the Hill coefficient. The data were also analyzed using the linearized form of eq 4, shown in eq 5, where $f = k_2/k_{2,max}$, $k_{1,app}/k_{1,app,max}$, or $K_{D,min}/K_D$ (*13*):

$$\log[f/(1 - f)] = \alpha_H \log [Mg^{2+}] + b \quad (5)$$

The pH dependence of the catalytic rate constant (k_2) for cleavage of 14-tRNA or 2′-deoxy-substituted 13-tRNA catalyzed by RNase P holoenzyme was analyzed assuming a single ionization, using eq 6.

$$k_2 = k_{max}/[1 + 10^{(pK - pH)}] \quad (6)$$

The dissociation constants of RNase P for $tRNA^{Asp}$ were determined (*28*) by fitting the gel filtration centrifuge column data to a standard binding isotherm (eq 7) in which the fraction of product or substrate bound ($[E{\cdot}L]/[L]_{total}$) was plotted against the enzyme concentration ($[E]_{total}$).

$$[E{\cdot}L]/[L]_{total} = 1/(1 + K_D/[E]_{total}) \quad (7)$$

For measurements of the binding of magnesium ion to RNase P RNA or holoenzyme, the proportion of magnesium

bound to RNase P ($[Mg^{2+}]_{bound}$) was calculated by subtracting ($[Mg^{2+}]_{free}$) from ($[Mg^{2+}]_{total}$). The data were analyzed by plotting υ ($[Mg^{2+}]_{bound}$/[RNase P]) against $[Mg^{2+}]_{free}$ and fitting to eq 8, assuming multiple, noninteracting sites (*13*):

$$\upsilon = (n[Mg^{2+}]_{free}/{K_{1/2}}^{Mg})/(1 + [Mg^{2+}]_{free}/{K_{1/2}}^{Mg}) \quad (8)$$

where n is the number of identical magnesium ion binding sites and ${K_{1/2}}^{Mg}$ is the apparent dissociation constant describing the affinity of these sites for magnesium. Data were also fit to eq 9, the linearized form of eq 8, commonly known as the equation for a Scatchard plot (*33, 35*).

$$\upsilon/[Mg^{2+}]_{free} = n/{K_{1/2}}^{Mg} - \upsilon/{K_{1/2}}^{Mg} \quad (9)$$

RESULTS

Binding of Magnesium to RNase P. Previous studies (*8*−*10*) have demonstrated that the protein component of RNase P decreases the concentration of magnesium ion required for optimal catalytic activity. This altered magnesium ion dependence is at least partially due to the enhanced affinity of the holoenzyme for pre-tRNA (*20, 21*). However, the protein component could also potentially enhance the affinity of magnesium ions bound to the holoenzyme. To test this, we directly measured the binding of magnesium ions to the RNase P holoenzyme. Previously, we measured binding of magnesium ions to P RNA using gel filtration centrifuge columns to separate the free and bound magnesium ions, and the fluorescent magnesium indicator, HQS, to quantify the magnesium concentration in each sample (*13*). At saturating magnesium concentrations, 90−130 magnesium ions cluster nonspecifically about the RNase P RNA to counter the strong Coulombic field associated with the polyanion. In contrast with measurements on tRNA (reviewed in *36*), Scatchard analysis of these data (*35*) fails to detect any higher affinity or cooperative magnesium ions, suggesting that such sites comprise at most a small minority (<10%) of the magnesium ions associated with P RNA.

To determine whether the addition of the protein component increases the apparent affinity of P RNA for magnesium ions, or promotes the formation of specific magnesium binding sites, we measured the binding of magnesium ions to RNase P in the presence and absence of the protein component. As previously observed for the binding of magnesium ions to RNase P RNA (*13*), a Scatchard plot of the magnesium binding data is linear (Figure 1, inset), providing no evidence for multiple classes of independent magnesium ion binding sites or cooperative magnesium ion sites (*35*). A plot of υ versus $[Mg^{2+}]_{free}$ is well described by eq 8, yielding estimates of the total number of sites, n = 150 ± 20, and ${K_{1/2}}^{Mg} = 0.26 \pm 0.06$ mM in the absence of added KCl (monovalent cation concentration ≈ 50 mM due to Tris cations and KOH added to adjust the pH; *32*), and n = 160 ± 30 and ${K_{1/2}}^{Mg} = 1.5 \pm 0.3$ mM upon the addition of 0.1 M KCl (Figure 1; total monovalent cation concentration ≈ 150 mM). Hill plots of the data indicate a lack of cooperativity as Hill coefficients (α_H) of ∼1 are observed (0.93 ± 0.07 and 0.96 ± 0.05 in the absence and presence of 0.1 M KCl, respectively) (data not shown). These data contrast with the magnesium-dependence of RNase P folding, where the apparent affinity is lower (${K_{1/2}}^{Mg}$ = 2−3 mM) and the cooperativity is increased (α_H = ∼3) (*16*). Furthermore, these data indicate that the protein component does not affect the apparent binding affinity of bulk magnesium ions to P RNA (Figure 1). Our value of ${K_{1/2}}^{Mg}$ is nearly identical to that previously observed for binding of magnesium to P RNA in the absence of added monovalent cations (${K_{1/2}}^{Mg}$ = 0.21 mM; *13*). The slightly higher value for n than previously observed (∼150 compared to ∼100) is likely due to an underestimation of n in the previous experiments due to the dissociation of weakly associated magnesium ions during the gel filtration step (*13*). Last, when we directly compared magnesium ion binding to RNase P RNA and holoenzyme, we obtained identical values of υ for a given $[Mg^{2+}]_{free}$ (Figure 1). Taken together, these results indicate that the protein subunit does not significantly affect the affinity or the number of magnesium ions that interact electrostatically with the P RNA polyanion.

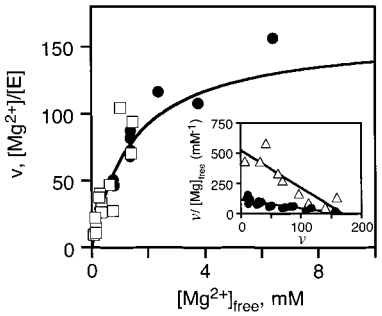

FIGURE 1: Binding of magnesium to RNase P in the presence and absence of the protein component as measured by the separation of free and bound magnesium using Microcon 30 ultrafiltration membranes, followed by quantification using the fluorophore 8-hydroxyquinoline-5-sulfonic acid (*13*). RNase P RNA (□) or holoenzyme (●) was incubated in Mes/Tris/Amp buffer (pH 8.0) with varying concentrations of $MgCl_2$ and a constant concentration (100 mM) of KCl. The data were plotted as υ (mol of Mg^{2+} bound/mol of RNase P) versus $[Mg^{2+}]_{free}$. A fit of the holoenzyme data to a binding isotherm (eq 8) yields estimates of n = 160 ± 30 (extrapolated at high $[Mg^{2+}]_{free}$) and ${K_{1/2}}^{Mg} = 1.5 \pm 0.3$ mM. The inset shows a Scatchard plot in which the data are plotted as $\upsilon/[Mg^{2+}]_{free}$ versus υ for RNase P holoenzyme in the presence (●) and absence (△) of 100 mM KCl.

tRNA^{Asp} Binding to RNase P. To pursue the possibility that the protein component alters the structure and magnesium ion binding affinity of localized regions of P RNA, we measured the effect of the protein component on the magnesium ion dependence of mature tRNA affinity. The affinity of P RNA for tRNA^{Asp} at high salt (∼1 M NH_4Cl) increases with magnesium ion concentration with a previously determined Hill coefficient of 1.9 ± 0.1 and a ${K_{1/2}}^{Mg}$ of 75 mM $MgCl_2$ (*13*). These data indicate that at least two magnesium ions bind more tightly to the P RNA·tRNA complex than to P RNA or tRNA alone.

To determine whether the protein component of the RNase P holoenzyme stabilizes magnesium ion sites that enhance tRNA binding, we compared the tRNA affinities of RNase P RNA and holoenzyme as a function of $MgCl_2$ concentration using gel filtration centrifuge columns to separate free and bound tRNA (*28*) (Figure 2). For measurements of the magnesium-dependence of binding and catalysis (shown below), the concentrations of magnesium chloride and potassium chloride were inversely varied to maintain a constant ionic strength. Under these conditions, the data are well described by a single binding isotherm (eq 7; Figure 2A). Furthermore, the tRNA dissociation constant (${K_D}^{tRNA}$,

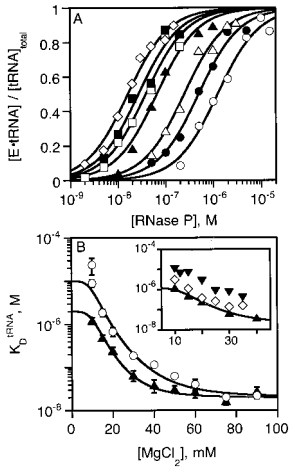

FIGURE 2: Measurement of the affinity of RNase P RNA or holoenzyme for mature $tRNA^{Asp}$. 5′-End-labeled mature $tRNA^{Asp}$ (0.1−1 nM) was incubated with a ≥5-fold molar excess of RNase P RNA or holoenzyme (2−2000 nM) in the presence of Mes/Tris buffer (pH 6.0) and 10−90 mM $MgCl_2$ and KCl varied (400−160 mM) to maintain constant ionic strength. The fraction of $tRNA^{Asp}$ bound to RNase P was monitored as the fraction of total radioactivity eluted from a G-75 Sephadex centrifuge column, and dissociation constants were determined by fitting a binding isotherm (eq 7) to these data. (A) Measurements of mature $tRNA^{Asp}$ binding to RNase P holoenzyme yielded the following dissociation constants: 75 mM $MgCl_2$ (◇), 16 ± 3 nM; 60 mM $MgCl_2$ (■), 27 ± 8 nM; 40 mM $MgCl_2$ (□), 39 ± 13 nM; 30 mM $MgCl_2$ (▲), 66 ± 18 nM; 20 mM $MgCl_2$ (△), 250 ± 50 nM; 15 mM $MgCl_2$ (●), 500 ± 80 nM; 10 mM $MgCl_2$ (○), 1300 ± 200 nM. (B) Dissociation constants for binding of mature $tRNA^{Asp}$ to RNase P RNA (○) or holoenzyme (▲) as a function of [$MgCl_2$]. Equation 11, derived from Scheme 2 (see Discussion), is fit to the data. The inset shows dissociation constants for binding of mature $tRNA^{Asp}$ to RNase P RNA (▼) or holoenzyme (◇) under low-salt conditions (10−35 mM $MgCl_2$, 100−25 mM KCl) compared with binding to RNase P holoenzyme under intermediate salt conditions (▲).

Scheme 1[a]

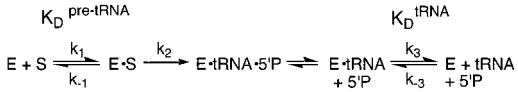

[a] E = RNase P RNA or holoenzyme; S = pre-$tRNA^{Asp}$; 5′P = 5′-leader sequence.

Scheme 1) decreases with magnesium ion concentration for both RNase P RNA and holoenzyme (Figure 2B). The affinity of the holoenzyme for tRNA is modestly enhanced (3−10-fold) compared to P RNA at low to moderate concentrations of $MgCl_2$ (10−50 mM) while at saturating magnesium ion concentrations the data converge on a similar maximum affinity ($K_{D,min}^{tRNA}$) of 10−15 nM (Figure 2B). The data do not provide strong evidence that RNase P binds tRNA in the absence of magnesium ions; therefore, the tRNA affinity at low magnesium ion concentration, shown in Figure 2B, is a lower limit for this parameter (see Discussion).

A Hill plot of the dependence of K_D^{tRNA} on $MgCl_2$ concentration further demonstrates that the protein component has little effect on the affinity or the cooperativity of magnesium ions that enhance tRNA binding to RNase P [α_H = 3.4 ± 0.2 and 2.7 ± 0.4, and $K_{1/2}^{Mg}$ = 78 ± 12 and 53 ± 13 for RNase P RNA (Figure 6B) and holoenzyme (Table 1), respectively)]. This Hill coefficient of ∼3 is higher than previously reported (α_H ∼ 2; *13*), perhaps due to the substitution of the monovalent ammonium ion by potassium.

Table 1: Magnesium Dependence of Kinetic and Thermodynamic Parameters for RNase P Holoenzyme

kinetic parameters	substrate	α_H	$K_{1/2}^{Mg}$ (mM)	k_{max} or $K_{D,min}$	ionic strength (M)	pH
k_2	5-tRNA	−	<4	0.13 ± 0.02[a]	0.13[d]	6.0
k_2	4-tRNA	−	<4	0.16 ± 0.03[a]	0.13[d]	6.0
k_2	3-tRNA	4.1 ± 0.9	4.6 ± 0.2	0.21 ± 0.01[a]	0.13[d]	6.0
k_2	2-tRNA	3.6 ± 0.8	10 ± 1	0.25 ± 0.03[a]	0.13[d]	6.0
k_2	2-tRNA	4 ± 1	6.6 ± 0.5	0.48 ± 0.04[a]	0.43[e]	6.0
k_2	1-tRNA	3.4 ± 0.6	10 ± 1	0.19 ± 0.01[a]	0.43[e]	6.0
k_2	1-tRNA	4 ± 1	12 ± 1	0.039 ± 0.001[a]	0.43[e]	5.2
K_D	tRNA	2.7 ± 0.4	53 ± 13	15 ± 4[b]	0.43[e]	6.0
K_D	1-tRNA	3.8 ± 0.5	∼30	160[b]	0.43[e]	5.2
$k_{1,app}$	1-tRNA	4.9 ± 0.9	∼30	0.22[c]	0.43[e]	5.2

[a] s^{-1}. [b] nM. [c] μM^{-1} s^{-1}. [d] 50 mM Mes, 50 mM Tris, 4−35 mM $MgCl_2$, 118−25 mM KCl, 37 °C. [e] 50 mM Mes, 50 mM Tris, 5−90 mM $MgCl_2$, 415−160 mM KCl, 37 °C.

Scheme 2[a]

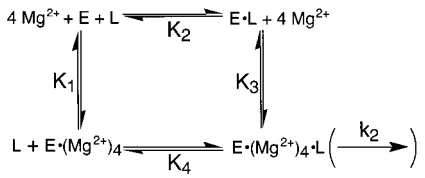

[a] E = RNase P RNA or holoenzyme; L (ligand) = pre-$tRNA^{Asp}$ or mature $tRNA^{Asp}$.

Both sets of data are well described by a model in which 3−4 magnesium ions bind completely cooperatively to the RNase P•tRNA complex (Scheme 2 and Discussion) with higher affinity than to either RNase P or tRNA. Other, more complicated models (e.g., including >4 cooperative magnesium sites or 4 noninteracting sites) can also describe the data; however, this is the simplest model consistent with the data.

Additional K_D^{tRNA} measurements were performed at low salt concentrations (ionic strength = 130 mM), our standard conditions for measuring holoenzyme kinetics (*20*, *21*) (Figure 2B, inset). The protein component modestly decreases the dependence of K_D^{tRNA} on ionic strength; dissociation constants increase by a factor of about 4-fold for P RNA when the ionic strength decreases from 430 to 130 mM, while for holoenzyme the increase is only about 2-fold. Thus, the protein slightly enhances tRNA binding affinity at low salt, but continues to have little effect on $K_{1/2}^{Mg}$ (Figure 2B, inset). The similarity between RNase P RNA and holoenzyme in the cooperativity and affinity of the magnesium ion binding sites that enhance tRNA binding suggests that the protein component does not significantly alter the P RNA structure in the region that interacts with tRNA.

Effects of Magnesium Ion Concentration on Single-Turnover Kinetics. To further investigate the role of the protein component in lowering the magnesium ion concentration required for efficient catalysis, we measured the magnesium ion dependence of the cleavage rate constant (k_2 in Scheme 1) by single-turnover kinetics. Previously, we demonstrated that RNase P holoenzyme cleaves pre-$tRNA^{Asp}$ substrates with a leader sequence ≥2 nucleotides in length by a kinetic mechanism of two consecutive, irreversible reactions in 10 mM $MgCl_2$, 100 mM NH_4Cl, pH 6 (*20*) (Scheme 1; $k_{-1} < k_2$). The hallmark of this mechanism is the appearance of lags in the timecourses of pre-tRNA

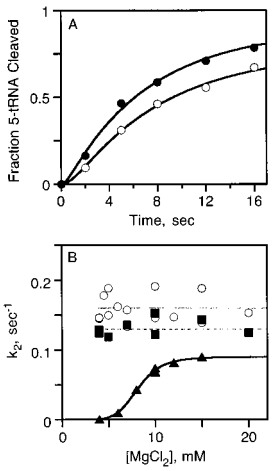

FIGURE 3: Measurement of the magnesium ion dependence of the cleavage rate constant (k_2) for substrates with leader sequences that are ≥4 nucleotides. 5′-End-labeled 4-, 5-, or 14-tRNA (0.2−10 nM) was incubated with high concentrations (5−10 μM) of RNase P holoenzyme in Mes/Tris buffer (pH 6.0) and varying concentrations of $MgCl_2$ with the ionic strength maintained by varying the [KCl]. The products of the reaction were analyzed as described under Materials and Methods. (A) The fraction of 5-tRNA cleaved over time (4−20 mM $MgCl_2$, 118−70 mM KCl) is well-described by the equation for two consecutive irreversible reactions (eq 1), yielding the following estimates of k_2: 0.13 ± 0.01 s^{-1}, 4 mM $MgCl_2$ (○); and 0.14 ± 0.01 s^{-1}, 15 mM $MgCl_2$ (●). The differences in the fraction cleaved reflect mainly differences in k_1. (B) Dependence of k_2 on [$MgCl_2$] for cleavage of 4-tRNA (○) and 5-tRNA (■) by RNase P holoenzyme, compared to the magnesium dependence of k_2 for cleavage of 5-tRNA by RNase P RNA at low salt (▲; 4−15 mM $MgCl_2$, 118−85 mM KCl). Dashed lines indicate the mean values of k_2 for holoenzyme-catalyzed cleavage of 4-tRNA (long dashes, 0.16 ± 0.03 s^{-1}) and 5-tRNA (short dashes, 0.13 ± 0.02 s^{-1}). The Hill equation (eq 4) was fit to the RNase P RNA data.

cleavage catalyzed by intermediate enzyme concentrations (k_1[E] ≈ k_2). For substrates containing a 4 nucleotide (4-tRNA; 5′-GCAU-tRNA^{Asp}), 5 nucleotide (5-tRNA; 5′-GACAU-tRNA^{Asp}) (Figure 3A), or 14 nucleotide (14-tRNA; 5′-GGUACCCAAAACAU-tRNA^{Asp}) leader sequence, the data are well described by this mechanism. Furthermore, the rate constant at saturating RNase P concentration (k_2) is unaffected by varying the $MgCl_2$ concentration from 4 to 20 mM; the mean values of the observed rate constants are 0.16 ± 0.03 s^{-1} for 4-tRNA and 0.13 ± 0.02 s^{-1} for 5-tRNA (Figure 3B), and 0.11 ± 0.02 s^{-1} for 14-tRNA (data not shown). When the $MgCl_2$ concentration is less than 4 mM, the measurement of k_2 is complicated by the magnesium ion-dependent unfolding of RNase P RNA (*16*) and the uncertainty in the free magnesium ion concentration due to magnesium ion depletion by high nucleic acid (P RNA) concentrations (*13*). Increasing the ionic strength to 430 mM increases k_2 for cleavage of 5-tRNA to 0.31 ± 0.03 s^{-1}; however, k_2 remains magnesium-independent (4−50 mM $MgCl_2$) so $K_{1/2}^{Mg}$ remains <4 mM (data not shown). However, the apparent association rate constant (k_1) for 5-tRNA cleavage does decrease as the magnesium ion concentration is lowered from 10 mM (100 mM KCl; k_1 = 3.6 ± 0.3 μM^{-1} s^{-1}) to 4 mM (118 mM KCl; k_1 = 0.9 ± 0.3 μM^{-1} s^{-1}) (data not shown). Previously, the magnesium ion dependence for cleavage of pre-tRNA by P RNA at high salt has been shown to depend on one or more (α_H = 1−3) weakly bound magnesium ions ($K_{1/2}^{Mg}$ ≥ 20 mM) (*13*, *17*, *37*). Since $K_{1/2}^{Mg}$ of k_2 for cleavage of pre-tRNA catalyzed by the holoenzyme is less than 4 mM, this suggests that one role of the protein component is to increase the affinity of RNase P·pre-tRNA for at least one catalytic magnesium ion.

To directly compare RNase P RNA and holoenzyme-catalyzed cleavage of the same substrate under identical conditions, we measured the magnesium ion dependence of k_2 for cleavage of 5-tRNA catalyzed by P RNA at low monovalent cation concentrations. Compared to the previous measurements at high monovalent concentrations (*13*, *17*, *37*), at ∼0.1 M KCl both the apparent magnesium ion affinity ($K_{1/2}^{Mg}$ = 8.2 ± 0.1 mM, Figure 3B) and the Hill coefficient (α_H = 6.5 ± 0.6) are considerably higher. Increasing the ionic strength to 430 mM with added KCl increases k_{max} (from 0.09 ± 0.01 to 0.16 ± 0.01 s^{-1}) but does not enormously affect $K_{1/2}^{Mg}$ (8.6 ± 0.2 mM) or α_H (5.2 ± 0.5) (data not shown). Therefore, the increased Hill coefficient compared to previous measurements is not due simply to a variation in the ionic strength, but likely reflects both the altered monovalent composition (K^+ versus NH_4^+ or Na^+) and the differences in the length of the 5′-leader sequence (5 nucleotides versus 33 nucleotides). These results suggest that at least five magnesium ions stabilize the transition state for cleavage of 5-tRNA relative to the P RNA·5-tRNA ground-state complex. These magnesium ions could enhance P RNA·5-tRNA cleavage either directly, by interacting with the transition state, or indirectly, by stabilizing the structures of one or both RNAs. Although we were not able to measure a Hill coefficient for the magnesium dependence of cleavage of 5-tRNA by holoenzyme, measurements with other substrates (see below) suggest that the cooperativity is lower for the holoenzyme.

Magnesium Ion Dependence of Pre-tRNA Substrates with Short Leaders. Previous studies have demonstrated that the protein component of RNase P enhances pre-tRNA affinity by directly interacting with nucleotides in the 5′-leader sequence of the substrate (*20*, *22*). 2-tRNA binds to the *B. subtilis* holoenzyme 10-fold more tightly than mature tRNA, and an additional three nucleotides (5-tRNA) increase binding affinity by an additional 40-fold in 10 mM $CaCl_2$, 100 mM NH_4Cl (*20*). To determine whether the direct protein/pre-tRNA contact is coupled to the enhanced magnesium affinity, we measured the magnesium ion dependence of k_2 for the holoenzyme-catalyzed cleavage of substrates with short (one, two, or three nucleotide) leader sequences.

A mechanism of two consecutive, irreversible first-order reactions describes the cleavage of 2-tRNA (Figure 4, inset) and 3-tRNA (data not shown). The cleavage rate constants at saturating enzyme (0.25 ± 0.03 s^{-1} for 2-tRNA, and 0.21 ± 0.01 s^{-1} for 3-tRNA) are slightly faster than those observed for substrates with longer leaders. However, the concentration of magnesium ions required to achieve the optimal cleavage rate constant is increased: $K_{1/2}^{Mg}$ = 10 ± 1 mM for 2-tRNA, while $K_{1/2}^{Mg}$ = 4.6 ± 0.2 mM for 3-tRNA (Figure 4; Table 1). Increasing the ionic strength enhances the cleavage rate constant and decreases $K_{1/2}^{Mg}$ up to 2-fold, but does not affect α_H (Table 1). The observed increases in $K_{1/2}^{Mg}$ for cleavage of 2- and 3-tRNA compared to longer substrates parallel the increases in K_D for pre-tRNA (*20*), but the Hill coefficient, reflecting the minimal number of specific magnesium ion binding sites, does not change (α_H = 3.6 ± 0.8 for 2-tRNA and 4.1 ± 0.9 for 3-tRNA). These data suggest that the direct

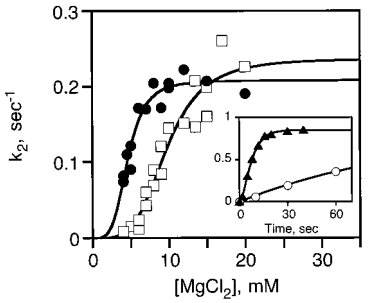

FIGURE 4: Magnesium ion dependence of k_2 for cleavage of 2-tRNA at constant ionic strength (□; 4−20 mM $MgCl_2$, 118−70 mM KCl) and 3-tRNA (●; 3−20 mM $MgCl_2$, 121−70 mM KCl) catalyzed by the RNase P holoenzyme. Equation 12 (see Discussion) was fit to the data to obtain estimates of K_3 (Scheme 2), the dissociation constant for the binding of magnesium to E·2-tRNA [9 (±2) × 10^{-9} M^4], or E·3-tRNA [4.5 (±0.7) × 10^{-10} M^4]. The inset shows representative timecourses for cleavage of 2-tRNA at 4 mM $MgCl_2$ (○; 0.009 ± 0.002 s^{-1}) and 15 mM $MgCl_2$ (▲; 0.21 ± 0.05 s^{-1}). A minimum of six time points was determined for each curve.

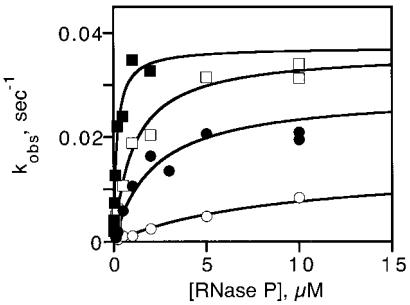

FIGURE 5: Cleavage of 1-tRNA catalyzed by the RNase P holoenzyme at constant ionic strength. 5′-End-labeled 1-tRNA (0.2−10 nM) was incubated with excess concentrations of RNase P holoenzyme (2 nM−20 μM P RNA, 22 nM−20 μM P protein) in the presence of Mes/Tris buffer (pH 5.2 or 6.0) containing 5−50 mM $MgCl_2$ and 415−280 mM KCl. Timecourses for cleavage of 1-tRNA were well-described by a single-exponential (eq 2). Equation 3, derived for a rapid equilibrium kinetic mechanism, was fit to the dependence of k_{obs} on RNase P holoenzyme concentration to obtain estimates of k_2, K_D^{1-tRNA}, and $k_{1,app}$. Representative plots (pH 5.2) at various magnesium ion concentrations are: 10 mM $MgCl_2$, 400 mM KCl (○) [k_2 = 0.015 ± 0.001s^{-1}, K_D^{1-tRNA} = 9 ± 2 μM, $k_{1,app}$ = 1.6 ± 0.2 mM^{-1} s^{-1}]; 15 mM $MgCl_2$, 385 mM KCl (●) [k_2 = 0.028 ± 0.003 s^{-1}, K_D^{1-tRNA} = 2.1 ± 0.7 μM, $k_{1,app}$ = 13 ± 3 mM^{-1} s^{-1}]; 20 mM $MgCl_2$, 370 mM KCl (□) [k_2 = 0.036 ± 0.002 s^{-1}, K_D^{1-tRNA} = 1.1 ± 0.2 μM, $k_{1,app}$ = 33 ± 4 mM^{-1} s^{-1}]; and 40 mM $MgCl_2$, 310 mM KCl (■) [k_2 = 0.037 ± 0.002 s^{-1}, K_D^{1-tRNA} = 0.18 ± 0.04 μM, $k_{1,app}$ = 210 ± 30 mM^{-1} s^{-1}].

protein/pre-tRNA contacts between the leader sequence and the protein central cleft (*22*) enhance both the affinity of pre-tRNA and the affinity of the magnesium ions bound to the RNase P·pre-tRNA complex.

The previous kinetic data and tRNA binding data suggest that multiple magnesium ions (a minimum of 3−4 for binding and 4 for cleavage) participate in the reaction catalyzed by the RNase P holoenzyme. To test the total number of magnesium ions required for binding and cleaving pre-tRNA, we varied the substrate and reaction conditions to alter the kinetic mechanism to rapid equilibration of substrate binding ($k_{-1} > k_2$) followed by a slow cleavage step (*20*). For a rapid equilibrium mechanism, the holoenzyme concentration dependence of k_{obs} (Figure 5) simultaneously measures the pre-tRNA dissociation constant, K_D, the cleavage rate constant, k_2, and the apparent second-order

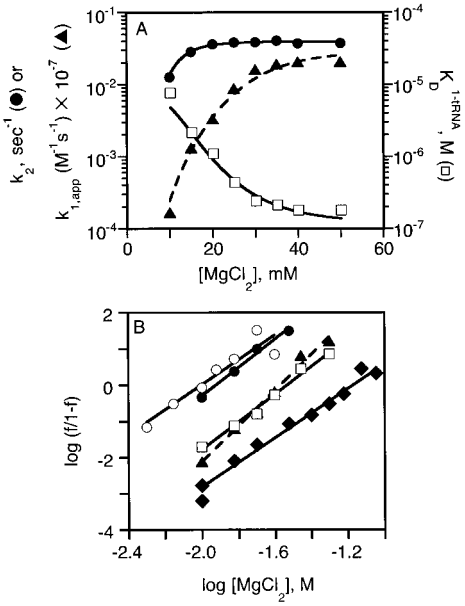

FIGURE 6: Magnesium dependence of 1-tRNA cleavage catalyzed by RNase P holoenzyme at constant ionic strength. (A) Plot of kinetic parameters k_2 (●), K_D^{1-tRNA} (□), and $k_{1,app}$ (▲) versus $MgCl_2$ concentration at pH 5.2 (10−50 mM $MgCl_2$, 400−280 mM KCl). Equation 12 was fit to the magnesium dependence of k_2 to obtain an estimate of K_3, the dissociation constant for the binding of magnesium to E·1-tRNA in Scheme 2 [2.0 (±0.3) × 10^{-8} M^4]. This value of K_3 was used in eq 11 to describe the magnesium-dependent decrease in K_D^{1-tRNA}. The $k_{1,app}$ data were fit using the Hill equation (eq 4) with α_H = 4. (B) Hill plots illustrating the cooperativity of the magnesium dependence of the following kinetic parameters: k_2 at pH 6.0 (○); and k_2 (●), K_D^{1-tRNA} (□), and $k_{1,app}$ (▲) at pH 5.2 (slopes, α_H, are listed in Table 1). The Hill plots were derived as described under Materials and Methods using the limiting values at saturating magnesium concentrations for each kinetic parameter ($k_{2,max}$, $K_{D,min}^{1-tRNA}$, and $k_{1,app,max}$) to calculate f. The values of $k_{2,max}$ used for these plots are listed in Table 1. Estimates of 160 nM and 0.22 μM^{-1} s^{-1} (50 mM $MgCl_2$) were used to approximate $K_{D,min}^{1-tRNA}$ and $k_{1,app,max}$, respectively. Also shown is the Hill plot for the magnesium dependence of mature tRNA binding (K_D^{tRNA}) to RNase P RNA (◆) (slope = 3.4 ± 0.2).

rate constant, $k_{1,app}$. To achieve a rapid equilibrium mechanism, we used a substrate with a single-nucleotide leader (1-tRNA; 5′-U-$tRNA^{Asp}$) which binds 150-fold weaker than 2-tRNA and therefore increases the dissociation rate constant (k_{-1}) (*20*). Additionally, we lowered the pH from 6 to 5.2, which decreases k_2 from 0.2 to 0.04 s^{-1} without significantly altering the magnesium ion dependence of k_2 (Table 1) or the value of K_D^{1-tRNA} (data not shown). Under these conditions, no lags are observed even at 50 mM $MgCl_2$, indicative of a rapid equilibrium mechanism. Therefore, we measured the magnesium ion dependence of cleavage of 1-tRNA at pH 5.2 (Figure 6).

The value of k_2 at saturating magnesium concentrations (Figure 6A; Table 1) for cleavage of 1-tRNA decreases approximately 2-fold compared to cleavage of 2-tRNA under similar conditions (k_2 = 0.08 ± 0.01 s^{-1} in 15 mM $MgCl_2$, 385 mM KCl, pH 5.2; data not shown). The $K_{1/2}^{Mg}$ of 12 ± 1 mM, obtained from a Hill plot of the magnesium ion dependence of k_2 (Figure 6B), is nearly 2-fold higher than that observed for 2-tRNA at the same ionic strength, but α_H is essentially identical (Table 1). This Hill coefficient is consistent with our previous observations suggesting a minimal requirement of 4 specific magnesium ions for

Scheme 3[a]

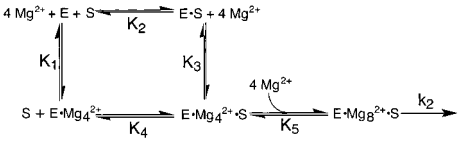

[a] E = RNase P holoenzyme; S = pre-tRNA^{Asp}.

cleavage of pre-tRNA by RNase P. Moreover, the observed $K_{1/2}^{Mg}$ continues the trend of decreasing magnesium ion affinity with decreasing E•pre-tRNA stability.

The magnesium ion dependence of K_D^{1-tRNA}, with a Hill coefficient of 3.8 ± 0.5 and $K_{1/2}^{Mg} \sim 30$ mM (Figure 6B), suggests that at least 4 magnesium ions stabilize the E•1-tRNA complex, as depicted in Scheme 2. Hence, the 1-tRNA data indicate that multiple magnesium ions are required for both pre-tRNA binding and catalysis (at least 4 for binding and at least 4 for catalysis). Two limiting models that explain these data are possible: (i) the same magnesium ion sites mediate both binding and catalysis, but their affinities are increased with binding of the substrate (Scheme 2); and (ii) distinct magnesium ion binding sites exist for binding and catalysis (Scheme 3). We can differentiate these two models by examining the magnesium ion dependence of the apparent second-order rate constant ($k_{1,app}$) for cleavage of 1-tRNA catalyzed by RNase P. For a rapid equilibrium mechanism, $k_{1,app}$ is not a true second-order rate constant, but instead equals k_2/K_D; thus, the magnesium ion dependence of this kinetic parameter reflects both the binding and catalytic steps in the kinetic mechanism. For cleavage of 1-tRNA catalyzed by the holoenzyme in 20 mM $MgCl_2$, the nearly 10-fold decrease in $k_{1,app}$ (from 0.32 ± 0.03 to 0.033 ± 0.004 μM^{-1} s^{-1}) as the pH is lowered from 6 to 5.2 confirms that this rate constant reflects cleavage in addition to binding.

Like K_D^{1-tRNA}, $k_{1,app}$ is also cooperatively dependent on the magnesium ion concentration, with a Hill coefficient of 4.9 ± 0.9 and $K_{1/2}^{Mg} \sim 30$ mM (Figure 6B). This Hill coefficient is smaller than the predicted $\alpha_H \approx 8$ for the magnesium ion dependence of $k_{1,app}$ if four distinct magnesium sites stabilize binding and catalytic steps (for a total of eight, Scheme 3). Taken together with the magnesium ion dependence of k_2 for cleavage of substrates with 1-, 2-, and 3-nucleotide 5′-leaders, these results suggest a lower limit of four *total* magnesium ions required to stabilize both binding *and* cleavage of pre-tRNA catalyzed by the RNase P holoenzyme (as in Scheme 2). Additionally, the protein component enhances the apparent affinity ($K_{1/2}^{Mg}$) of these magnesium ions, but does not increase the number of magnesium ion binding sites, as reflected by the Hill coefficient. This enhanced magnesium affinity correlates with the interaction of the protein component with the 5′-leader sequence, since $K_{1/2}^{Mg}$ decreases incrementally as the 5′-leader length increases from one to four nucleotides.

pH Dependence of Pre-tRNA Cleavage. Previously, Smith and Pace (*17*) used single-turnover kinetics to measure the pH dependence of k_2 for *E. coli* P RNA-catalyzed cleavage of *B. subtilis* pre-tRNA^{Asp} in 50 mM $CaCl_2$, 1 M NaCl. These data can be described by a single ionization, p$K_a \sim 8.5$, with maximal activity at high pH. The origin of this ionization is unclear; however, this pK_a has been proposed to reflect the ionization of a water molecule that may function as the nucleophile in the cleavage reaction (*2*, *17*), possibly

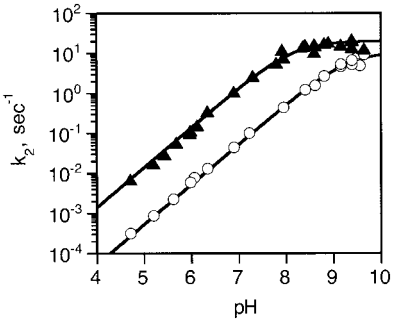

FIGURE 7: pH dependence of the cleavage rate constant (k_2) catalyzed by RNase P holoenzyme. 5′-End-labeled 14-tRNA^{Asp} or 2′-deoxy-substituted (at the cleavage site) 13-tRNA^{Asp} (0.2−10 nM) was incubated with RNase P (2−10 μM P RNA, 2−10 μM P protein) in 10 mM $MgCl_2$ and 100 mM KCl (37 °C). The pH was varied using a series of buffer mixtures of constant ionic strength (*32*), as described under Materials and Methods. The products of the single-turnover reactions were analyzed as described under Materials and Methods; at least six points were determined for each timecourse. Values of k_2 for 14-tRNA^{Asp} (▲) and 2′-deoxy-substituted 13-tRNA^{Asp} (○) were plotted as a function of pH. Equation 6 describing a single ionization was used to fit both the 14-tRNA ($k_{2,max} = 20 \pm 4$ s^{-1}, p$K_a = 8.2 \pm 0.2$) and the 2′-deoxy data ($k_{2,max} = 11 \pm 4$ s^{-1}, p$K_a = 9.3 \pm 0.4$).

stabilized by coordination to a magnesium ion (*24*). A number of structure-probing experiments suggest that the protein is localized near the active site of RNase P (S. Niranjanakumari, J. J. Day, and C. A. Fierke, unpublished results; *20*, *38*, *39)*. Therefore, the protein is positioned such that it could alter the pK_a of crucial active site residues.

To further define the function of the protein component in RNase P, we have investigated the pH dependence of k_2 for cleavage of 14-tRNA catalyzed by the RNase P holoenzyme under single-turnover conditions using buffer mixtures (see Materials and Methods) that vary the pH (4.7 to 9.7), while maintaining a constant ionic strength (*32*). The cleavage rate constant (k_2) was determined by fitting a single-exponential decay (eq 2) to the fraction of pre-tRNA cleaved over time (data not shown). The dependence of k_2 on pH is well-described by a single ionization with a pK_a of 8.2 ± 0.2 and a pH-independent rate constant (k_{max}) of 20 ± 4 s^{-1} at high pH (Figure 7), suggesting that the protein component has no large effect on this apparent ionization.

Free hexaaquo Mg^{2+} ionizes with a pK_a of 11.4, and the pK_as of the ionizable groups of nucleotides are ≥10 (*40*); hence, a catalytic pK_a of 8−8.5 could suggest that both RNase P RNA and holoenzyme greatly stabilize the ionized species. To test whether our measurements truly reflect the thermodynamic ionization, we measured the pH dependence of the holoenzyme-catalyzed cleavage rate constant for a substrate that is cleaved more slowly, a 13-tRNA containing a 2′-deoxy substitution at the cleavage site (Figure 7). As expected (*16)*, the cleavage rate constant of this 2′-deoxy substrate is 20−25-fold slower than cleavage of the native substrate at neutral pH. However, the pH dependence of the cleavage rate constant for 2′-deoxy 13-tRNA is well-described by a $k_{max} = 11 \pm 4$ s^{-1}, which is ≤2-fold lower than the pH-independent rate constant for the native substrate, and a pK_a of 9.3 ± 0.4 (the errors in these parameters are increased as the highest pH measured was 9.7). These data indicate either that the 2′-hydroxyl group adjacent to the cleavage site is important for lowering the pK_a of the ionizing

group or that the measured pK_a is "kinetically perturbed" (*24*), reflecting a change in the rate-limiting step rather than an alteration in the thermodynamic pK_a.

Competition by Cobalt(III) Hexammine. To further elucidate the function of catalytically important magnesium ions in RNase P, we investigated the effect of cobalt(III) hexammine [$Co(NH_3)_6^{3+}$] on catalysis. Cobalt hexammine has previously been used as a probe of outer-sphere $Mg(H_2O)_6^{2+}$ binding sites because the two complexes share similar size and hydrogen-bonding properties, but the amine ligands of cobalt hexammine do not dissociate or ionize (*26*). Not surprisingly, given the sheer number of magnesium ions that bind to RNase P, and their potentially varied roles and binding modes, the activity of RNase P holoenzyme is decreased more than 10^6-fold in the presence of 10 mM $Co(NH_3)_6^{3+}$ alone (100 mM KCl, pH 7.8; data not shown). *E. coli* RNase P RNA is also inactive in the presence of $Co(NH_3)_6^{3+}$ alone (*41*). Given the similarities between $Co(NH_3)_6^{3+}$ and $Mg(H_2O)_6^{2+}$ (*26*), this result is most simply explained by a model in which cobalt hexammine functionally substitutes for most nonspecific and outer-sphere magnesium ions, but only displaces (does not substitute for) magnesium ions in roles that require the ionization or the displacement of at least one H_2O from the magnesium hydration shell. However, recent structural studies of the P4−P6 domain of the self-splicing *Tetrahymena thermophila* intron (*42*) indicate that hexahydrated magnesium and cobalt hexammine binding sites are not coincident. Therefore, this inhibition could also be due to loss of an essential outer-sphere magnesium binding site or a novel cobalt hexammine binding site.

In the presence of saturating concentrations of $MgCl_2$ (Figure 8A), the addition of cobalt hexammine inhibits the single-turnover cleavage of 5-tRNA catalyzed by RNase P holoenzyme in a hyperbolic manner ($K_{I,app} = 0.31 \pm 0.02$ mM at 5 mM $MgCl_2$ and 0.64 ± 0.09 mM at 10 mM $MgCl_2$). Interestingly, the magnesium ion dependence of k_2 for cleavage of 5-tRNA is hyperbolic ($\alpha_H = 1$) in the presence of cobalt hexammine (Figure 8B). This is in contrast to the highly cooperative magnesium ion dependence of pre-tRNA cleavage catalyzed by RNase P in the absence of $Co(NH_3)_6^{3+}$ (Table 1). At higher concentrations of cobalt hexammine, the magnesium ion concentration required for saturation increases but $k_{2,max}$ is constant, indicating that cobalt hexammine acts as an inhibitor that is competitive with one class of magnesium sites (Figure 8A, inset, and Figure 8B). These data suggest that $Co(NH_3)_6^{3+}$ functionally replaces all but one class of the magnesium ions that stabilize pre-tRNA cleavage and/or the active structure of P RNA.

The equation for competitive inhibition (eq 10) may be used to simultaneously fit the dependence of k_2 on [Mg^{2+}] and [$Co(NH_3)_6^{3+}$] using the program Systat 5.2 (Systat, Inc.):

$$k_{2,obs} = k_{2,max}[Mg^{2+}]/\{[Mg^{2+}] + K_{app}^{Mg}(1 + [Co(NH_3)_6^{3+}]/K_I\} \quad (10)$$

where K_{app}^{Mg} is the apparent dissociation constant for magnesium in the absence of cobalt hexammine and K_I is the inhibition constant for cobalt hexammine. The K_{app}^{Mg} of 1.9 ± 0.1 mM derived from this analysis presumably reflects the apparent affinity of the magnesium binding site, or class

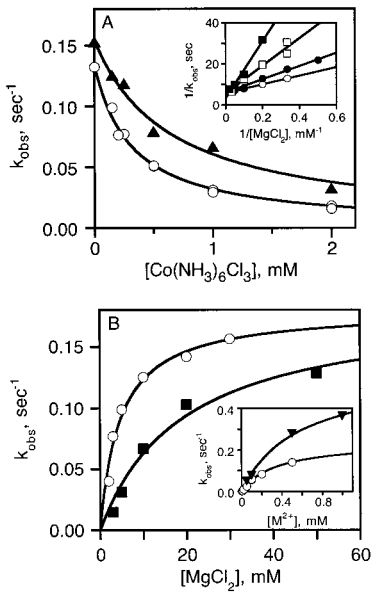

FIGURE 8: Competitive inhibition of holoenzyme-catalyzed 5-tRNA cleavage by cobalt(III) hexammine [$Co(NH_3)_6^{3+}$]. Single-turnover reactions were performed in Mes/Tris buffer (pH 6.0) containing 2−100 mM $MgCl_2$, 100 mM KCl, saturating (0.16−5 μM) holoenzyme, and 0.15−1.0 mM $Co(NH_3)_6^{3+}$. The k_{obs} values at 5 (○) and 10 mM $MgCl_2$ (▲) as a function of [$Co(NH_3)_6^{3+}$] are well-described by the equation $k_{obs} = k_0/(1 + [Co(NH_3)_6^{3+}]/K_{I,app})$, where k_0 is the cleavage rate constant in the absence of cobalt(III) hexammine and $K_{I,app}$ is an apparent inhibition constant, yielding $K_{I,app} = 0.31 \pm 0.02$ and 0.64 ± 0.09 for 5 and 10 mM $MgCl_2$, respectively. The inset shows a double-reciprocal plot of the magnesium ion dependence of k_{obs} at the following cobalt(III) hexammine concentrations: 0.15 mM (○), 0.25 mM (●), 0.5 mM (□), and 1.0 mM (■). (B) Magnesium dependence of k_{obs} is well-described by a hyperbola $\{k_{obs} = k_{max}[Mg^{2+}]/(K_{1/2}^{Mg} + [Mg^{2+}])\}$ for 0.15 mM (○, $k_{max} = 0.18 \pm 0.01$ s^{-1}, $K_{1/2}^{Mg} = 4.7 \pm 0.9$ mM) and 1.0 mM (■, $k_{max} = 0.18 \pm 0.03$ s^{-1}, $K_{1/2}^{Mg} = 19 \pm 6$ mM) cobalt(III) hexammine. Inset: In the presence of 2 mM cobalt(III) hexammine, k_{obs} is hyperbolically dependent on manganese (▼, pH 8, $K_{1/2} = 0.6 \pm 0.1$ mM) and zinc (○, pH 7, 0.4 ± 0.1 mM).

of sites, that is competitive with cobalt hexammine. These data do not readily distinguish a specific magnesium binding site ($K_{1/2}^{Mg} < 4$ mM, as measured by single-turnover kinetics) from nonspecific magnesium interactions ($K_{1/2}^{Mg} = 1.5$ mM, as measured by equilibrium dialysis). The K_I of 0.11 ± 0.01 mM suggests that cobalt hexammine associates with ~20-fold higher affinity to this (these) site(s) than magnesium ion (assuming $K_I \approx K_D$), consistent with values measured in other systems (*43*−*45*).

Substitution of Other Metals for Magnesium Ion. Previous studies demonstrated that the divalent magnesium and manganese ions can be used as cofactors by RNase P RNA and holoenzyme to catalyze efficient cleavage of native pre-tRNA substrates (*46*−*48*). Furthermore, calcium ions promote binding of substrate and product, but k_2 is reduced by several orders of magnitude (*21*, *46*). To further investigate the role of metals in pre-tRNA cleavage catalyzed by the holoenzyme, we measured the single-turnover activity in the presence of 100 mM KCl and various divalent cations. The *B. subtilis* holoenzyme (1 μM, pH 8) has very low cleavage activity in the presence of a 10 mM concentration of several metals [e.g., $CdCl_2$, $k_2 \sim 2 \times 10^{-5}$ s^{-1}; $CoCl_2$, $k_2 < 1 \times 10^{-6}$ s^{-1}; $ZnCl_2$, $k_2 \sim 4 \times 10^{-5}$ s^{-1}; $CaCl_2$, $k_2 = (9 \pm 2) \times 10^{-4}$ s^{-1}; data not shown]. However, in the presence of 2 mM $Co(NH_3)_6^{3+}$, small concentrations of transition metals

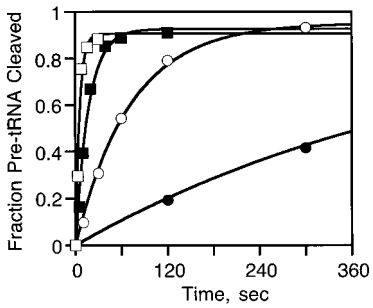

FIGURE 9: Holoenzyme-catalyzed cleavage of 14-tRNA in the presence of 2 mM $Co(NH_3)_6Cl_3$ and various alternative metals. Single-turnover rate constants were measured in Mes/Tris/Amp buffer, 2 mM $Co(NH_3)_6Cl_3$, and 100 mM KCl, with the following additions: 50 μM $PbCl_2$ (●), 0.0020 ± 0.0001 s^{-1} at pH 7.7; 50 μM $CdCl_2$ (○), 0.014 ± 0.001 s^{-1} at pH 7.9; 0.5 mM $CoCl_2$ (■), 0.057 ± 0.005 s^{-1} at pH 7.7; 0.2 mM $ZnSO_4$ (□), 0.18 ± 0.03 s^{-1} at pH 7.7.

(0.05−1 mM Pb^{2+}, Cd^{2+}, Co^{2+}, Mn^{2+}, and Zn^{2+}) stimulate pre-tRNA cleavage by 10^3-10^5-fold (Figure 9A and Figure 8B, inset). For all of these metals, the rate constant is pH-dependent under these conditions (data not shown), suggesting that the cleavage step is rate-limiting.

These data suggest that a variety of transition metals, in addition to magnesium, can compete with cobalt hexammine to stimulate the catalytic activity of the RNase P holoenzyme. To examine this further, we measured the single-turnover activity of RNase P in the presence of 2 mM cobalt hexammine and zinc or manganese (Figure 8B, inset). Under these conditions, the observed single-turnover rate constant shows a hyperbolic dependence on zinc(II) concentration where K_{app}^{Zn} (0.3 ± 0.1 mM) is not dependent on pH but $k_{2,max}$ increases with pH (from $k_{2,max} = 0.015 \pm 0.003$ s^{-1} at pH 5.6 to 0.25 ± 0.02 s^{-1} at pH 7.0; data not shown). Thus, zinc(II) activates cleavage at lower concentrations than magnesium(II) ($K_{app}^{Mg} > 20$ mM; data not shown) under these conditions, and the cleavage rate constant is only decreased about 5-fold compared to saturating magnesium ($k_{2,max}^{Mg} = 1.2$ s^{-1}, Figure 7). Manganese(II) similarly activates RNase P at a lower concentration ($K_{app}^{Mn} = 0.6 \pm$ 0.1 mM). These data demonstrate that zinc and manganese, but not cobalt(III) hexammine, can readily substitute for at least one magnesium ion essential for catalysis of pre-tRNA cleavage.

DISCUSSION

Nearly all RNase Ps, from all three domains of life (Archaea, Bacteria, and Eucarya) contain RNA *and* protein subunits essential to pre-tRNA processing in vivo (*1*−*3*). Most bacterial RNase P RNAs are catalytic in the absence of their cognate proteins in vitro, but these reactions require nonphysiologically high concentrations of monovalent and divalent cations to achieve catalytic efficiency comparable to the holoenzymes (*9*, *46*). Some archaeal RNase P RNA subunits are likewise sufficient for pre-tRNA processing, but require extreme conditions of up to 5 M ionic strength and display only marginal activity compared to their holoenzymes (*49*). These very substantial differences in salt optima suggest that the binding of the protein and magnesium ions, both essential cofactors in the reaction catalyzed by RNase P, are highly synergistic. The experiments described herein indicate that the protein component decreases the magnesium requirement for pre-tRNA cleavage catalyzed by RNase P by increasing the affinities of specific magnesium binding sites in the RNase P·pre-tRNA complex.

Effects of the Protein Component on Diffuse Mg^{2+} Binding. Magnesium ion interactions with RNA are classified into two distinct modes, diffusely bound and site-bound (*14*), either of which, in the case of RNase P RNA, could conceivably be affected by the presence of the protein component. The numbers and apparent affinities of diffusely bound cations are sensitive to the global charge density of the RNA (*14*). The protein subunit of RNase P could affect diffusely bound cations by: (i) countering the negatively charged phosphoribose backbone with several exposed basic residues (*23*) and thereby *decreasing* the overall charge density of P RNA; or (ii) inducing a conformational change that leads to a globally more compact RNA structure (*14*) which *increases* the charge density on P RNA. Additionally, the protein could stabilize a specific P RNA tertiary structure that could induce the formation of specific magnesium binding sites that could potentially be detected in nonlinear Scatchard plots, as observed for multiple classes of magnesium binding sites in tRNA (*50*−*53*).

The observed stoichiometry of magnesium ion binding to RNase P holoenzyme is 0.37 ± 0.05 Mg^{2+}/nucleotide (Figure 1), similar to that previously observed for binding of magnesium to tRNA and the hammerhead ribozyme (0.3−0.7 M^{2+}/nucleotide; summarized in *36*). Furthermore, this number is similar to the 0.44 M^{2+}/nucleotide for B DNA calculated from "counterion condensation" theory, which describes the purely electrostatic association of ions with polyelectrolytes based on the polyelectrolyte axial charge density (see reviews of counterion condensation theory in *54*−*57*). Additional evidence that the majority of these magnesium ions associate nonspecifically with RNase P is provided by the increase in the apparent binding constant for magnesium with increasing potassium concentration (Figure 1, inset) (*57*). Taken together with our previous results (*13*), these data demonstrate that the vast majority (>90%) of magnesium ions associate nonspecifically by electrostatic forces with both RNase P RNA and holoenzyme. Furthermore, these data indicate that the protein component does not affect the number and affinity of diffusely bound cations, providing no evidence for an alteration in the global RNA structure or the formation of a small number of high-affinity sites in RNase P RNA. These results are consistent with a variety of biophysical measurements (*15*, *16*, *58*−*61*) suggesting that RNA P RNA folds into a compact, native (or nearly native) structure under physiological salt conditions.

Effects of the Protein Component on Specific Mg^{2+} Sites That Enhance tRNA Binding. The protein subunit of RNase P also does not significantly alter the apparent number or cooperativity of specific magnesium binding sites that stabilize tRNA binding since a Hill coefficient of 3−4 is observed for both RNase P RNA and holoenzyme (Figure 2B). However, the protein modestly increases the affinity of RNase P for these magnesium ions, since $K_{1/2}^{Mg}$ decreases from ∼80 to ∼50 mM for the holoenzyme. The magnesium ion dependence of tRNA affinity can be described using a simple model where 4 magnesium ions bind completely cooperatively to stabilize the RNase P·tRNA complex

(Scheme 2). From this scheme, an equation quantitatively describing the dependence of $K_{D,obs}$ on magnesium ion concentration (eq 11) was derived:

$$K_{D,obs} = K_4([Mg^{2+}]^4 + K_1)/([Mg^{2+}]^4 + K_3) \quad (11)$$

where K_1 is the equilibrium constant for binding of magnesium ions to free E, K_3 is the equilibrium constant for binding of magnesium ions to E·L, and K_4 is the minimum K_D for tRNA or pre-tRNA at saturating magnesium concentrations. More complicated models, in which the four proposed magnesium ions bind to independent, nonidentical sites, could also explain the data, but this is the simplest model consistent with all of our current data.

Using Scheme 2, the value of K_4, the affinity of RNase P for tRNA at saturating magnesium concentration, can be estimated from K_D^{tRNA} at high magnesium (Figure 2B, $K_4 =$ 10−15 nM). The protein subunit does not alter this equilibrium constant significantly. The value of K_2, the affinity of RNase P for tRNA in the absence of bound magnesium ions, can theoretically be determined from the limiting affinity at low magnesium ion concentrations. However, binding measurements at low $[Mg^{2+}]$ are difficult due to aggregation and unfolding of RNase P under these conditions (*15*, *16*, *62*). Nonetheless, a lower limit for K_2 can be estimated from the tRNA affinity at 10 mM $MgCl_2$, $K_D^{tRNA} \geq 2\ \mu$M (holoenzyme) and $K_D^{tRNA} \geq 10\ \mu$M (P RNA). These values indicate that the bound magnesium ions enhance the affinity of RNase P for tRNA by more than 100-fold. Additionally, $K_{1/2}^{Mg}$, describing the magnesium ion dependent decrease in K_D^{tRNA} (Figure 2B), equals $(K_1 - 2K_3)^{1/4}$ (eq 12) which approximately equals $(K_1)^{1/4}$ (since $K_1 > K_3$). Therefore, $K_{1/2}^{Mg}$ mainly reflects K_1, the affinity of RNase P for magnesium ions, and the protein subunit modestly enhances the affinity of RNase P for these magnesium ions. However, these moderate effects of the protein component on the magnesium ion dependence of tRNA affinity are not sufficient to explain the functional effects of the protein in decreasing the overall magnesium ion requirement of RNase P.

Effects of the Protein Component on Specific Mg^{2+} Bound to E·Pre-tRNA. A comparison of the cleavage rate constant catalyzed by RNase P RNA and holoenzyme at saturating concentrations of magnesium ions (Figure 3B; *20*, *21*) demonstrates that the protein component does not enormously (<10-fold) enhance catalysis for pre-$tRNA^{Asp}$ substrates containing 5′-leaders of 2−33 nucleotides in length. Furthermore, the pH dependence of k_2 suggests that the protein component has no clear effect on the catalytic pK_a (Figure 7). However, the protein does influence the magnesium ion dependence of the single-turnover cleavage rate constant. In fact, the protein component decreases $K_{1/2}^{Mg}$ compared to both RNase P RNA-catalyzed cleavage of 33-tRNA at high salt (36 mM to <4 mM) (*13*) and cleavage of 5-tRNA at low salt (8 mM to <4 mM) (Figure 3B). Importantly, $K_{1/2}^{Mg}$ for the holoenzyme-catalyzed reaction is dependent on the length of the pre-tRNA 5′-leader, and the minimal $K_{1/2}^{Mg}$ is observed for a leader that is ≥4 nucleotides in length. This dependence of $K_{1/2}^{Mg}$ on leader length correlates with the previously observed leader length dependence of $K_D^{pre-tRNA}$ (*20*), where a 5 nucleotide leader is required for obtaining the maximal interaction with the RNase P holoenzyme. Additionally, a 4−5 nucleotide leader is required for optimal pre-tRNA/P protein cross-linking in an RNase P holoenzyme·pre-tRNA complex (*22*). These correlations suggest a linkage between the P protein/5′-leader interaction and the increased magnesium ion affinity.

The magnesium ion dependence of the cleavage rate constant (k_2) can be modeled as reflecting the relative concentrations of two ground-state complexes, E·pre-tRNA (inactive) and E·Mg_4·pre-tRNA (active) (see Scheme 2). This model can also be used to explain the effect of the protein component on the apparent magnesium affinity. The strongest evidence for a common set of magnesium binding sites stabilizing both pre-tRNA binding and cleavage is the similarity between the Hill coefficients for K_D^{1-tRNA}, k_2, and k_2/K_D^{1-tRNA} (Figure 6). The dependence of k_2 on magnesium ion concentration can be derived for Scheme 2 as

$$k_2 = k_{2,max}[Mg^{2+}]^4/(K_3 + [Mg^{2+}]^4) \quad (12)$$

In this model, $K_{1/2}^{Mg}$ for the observed single-turnover rate constant (the magnesium concentration at which $k_2 = k_{2,max}/2$) is equal to $(K_3)^{1/4}$. According to this simple model, therefore, the protein subunit decreases the magnesium requirement of RNase P by stabilizing the E·Mg_4·pre-tRNA ground state (and transition state) relative to the E·pre-tRNA complex. This conclusion assumes that the ground-state complexes E·pre-tRNA and E·Mg_4·pre-tRNA equilibrate rapidly compared to pre-tRNA cleavage (k_2), which is supported by the fact that $K_{1/2}^{Mg}$ for 1-tRNA does not decrease when the pH is lowered from 6.0 to 5.2. Therefore, all of our data are consistent with the model that the interaction between the protein component and the pre-tRNA 5′-leader sequence stabilizes the binding of magnesium ions to the E·pre-tRNA complex.

Possible Locations of Specific Mg^{2+} Binding Sites. Given that the protein component mainly enhances the apparent magnesium affinity of the E·pre-tRNA complex, we are tempted to conclude that these ions interact with the cleavage site and/or the 5′-leader sequence. However, since the Hill coefficient is the same, within error, for mature tRNA binding and for cleavage of 1-, 2-, and 3-tRNA, the data argue against additional magnesium ions interacting with the leader sequence. More likely, the interaction between the pre-tRNA leader and the RNase P protein enhances magnesium ion binding to the cleavage site, the mature tRNA domain, and/or P RNA.

Several studies provide evidence locating potential magnesium binding sites in the RNase P·pre-tRNA complex. Substitution of a sulfur atom for either the *pro-*R_P or the *pro-*S_P nonbridging oxygen (*63*−*66*) or the 3′-oxyanion leaving group (*67*) of the scissile phosphate in pre-tRNA decreases catalysis by >1000-fold, perhaps reflecting the disruption of a catalytic metal ion interaction. Furthermore, the inclusion of cadmium or manganese partially restores cleavage of the R_P-phosphorothioate-modified substrate catalyzed by RNase P RNA (*63*−*65*) or holoenzyme (*66*), suggesting that the *pro-*R_P oxygen may directly coordinate a metal ion in the transition state. R_P-Phosphorothioate substitutions elsewhere in the mature tRNA domain (*68*−*70*) have comparatively minor effects on binding or catalysis, suggesting that essential metals do not interact with these regions. Conversely, phosphorothioate modifications in

RNase P RNA that interfere with pre-tRNA cleavage occur in the core P4 helix (*71, 72*). R_P- and S_P-phosphorothioate modifications at positions A67, G68, or A352 in *E. coli* RNase P RNA (*73*) and homologous positions (A49 and G50) in *B. subtilis* P RNA (*74*) substantially decrease RNase P RNA and holoenzyme-catalyzed pre-tRNA cleavage. However, a direct role for metal ions in stabilizing the catalytic transition state has not yet been demonstrated unequivocally for any of these sites. Nevertheless, these data suggest that the strongest candidates for magnesium binding sites important for catalysis—and, therefore, likely to be sensitive to the protein component—are those metals that interact with pre-tRNA at the cleavage site phosphate and with P RNA at positions in the P4 helix.

Our results indicate that the enhancement in affinity of magnesium ion binding sites in P RNA and/or pre-tRNA is coupled to the P protein/5′-leader interaction in the RNase P holoenzyme·pre-tRNA complex. The affinity of RNA/Mg^{2+} sites could be indirectly enhanced by this interaction by the positioning of RNA ligands to more readily bind magnesium ion. Affinity-cleavage experiments using P protein site-specifically-labeled with hydroxyl-radical-generating reagents (S. Niranjanakumari, J. J. Day, and C. A. Fierke, unpublished results; *38*) demonstrate that amino acids in the conserved RNR-motif of the protein component mainly interact with helices P3 and P4 in the catalytic domain (*75*) of RNase P RNA. Thus, the protein component provides a secure anchor-point to immobilize the 5′-leader sequence relative to the P RNA catalytic domain. By anchoring the 5′-leader, the P protein/5′-leader interaction could enhance magnesium ion binding sites that are located between pre-tRNA and P RNA, or solely within P RNA.

The formation of many protein−RNA complexes is highly dependent on the magnesium concentration. For example, magnesium ions are essential for the binding of *Neurospora crassa* mitochondrial tyrosyl-tRNA synthetase to the isolated P4−P6 domain of mitochondrial group I introns (*18*) and for the recognition of 16S rRNA by ribosomal protein S4 from *Bacillus stearothermophilus* (*19*). In both of these cases, the binding of magnesium is proposed to stabilize the structure of the RNA that is recognized by the protein. In turn, the protein further organizes the RNA for subsequent function, either self-splicing or subunit assembly. In contrast, P protein binding does not significantly enhance the magnesium dependence of P RNA folding (*16*). Rather, the protein component enhances the magnesium affinity of the RNase P·pre-tRNA complex by positioning pre-tRNA and presumably inducing a specific RNA structure required for magnesium binding.

Possible Roles of Specific Mg^{2+} Elucidated by Metal-Substitution Experiments. Tertiary structural probing of *E. coli* P RNA by lead(II)-induced cleavage (0.5 mM Pb^{2+}, 100 mM NH_4Cl, pH 7.5) indicates that 5−10 mM Mg^{2+}, Mn^{2+}, Ca^{2+}, Sr^{2+}, or Ba^{2+} can induce nativelike P RNA structure, while Co^{2+}, Ni^{2+}, Zn^{2+}, Cu^{2+}, or Cd^{2+} induce only partial or no nativelike structure (*76*). Proper folding of P RNA, therefore, is apparently favored by the addition of "hard" metal ions (*77*) that can preferentially interact with phosphate oxygens, the least polarizable of the potential metal ligands in RNA. On the other hand, only manganese can substitute for magnesium to promote native structure and efficient cleavage of pre-tRNA substrates by RNase P (*9, 78*). The catalytic activity of RNase P is decreased enormously when magnesium ion is replaced by Ca^{2+}, Sr^{2+}, or Ba^{2+} (*21, 46−48, 78*), which are larger ions and have higher pK_as for the ionization of water ligands (*36*).

Cobalt(III) hexammine completely inhibits RNase P by competing with a single specific magnesium or class of magnesium binding sites (Figures 8 and 9). The K_I of 0.1 mM for cobalt hexammine inhibition of pre-tRNA cleavage catalyzed by RNase P is similar to the measured affinity of a variety of nucleic acids for $Co(NH_3)_6^{3+}$. For example, this K_I is similar to the dissociation constants (0.2−0.8 mM) measured for binding of cobalt hexammine to outer-sphere metal sites in the major grooves of RNA and A-form DNA (*79−81*). Furthermore, K_I and K_D^{Mg} (∼2 mM) for RNase P are very similar to the values determined for cobalt hexammine inhibition of HDV ribozyme catalysis (K_I = 0.045 mM, K_D^{Mg} = 2.4 mM) (*45*), where it is proposed to compete with, but not substitute for, the general-base activity of $Mg(H_2O)_5(OH)^+$. Metal binding to RNA hairpins suggests that $Co(NH_3)_6^{3+}$ can also compete with inner-sphere magnesium ion binding sites, but in this case the $Co(NH_3)_6^{3+}$ and magnesium ion binding affinities are similar (*80, 82−84*). These comparisons suggest that $Co(NH_3)_6^{3+}$ inhibits RNase P by displacing an essential outer-sphere magnesium ion, although recent structural studies of cobalt hexammine binding to RNA (*42*) suggest that the binding sites of the two metal ions (hexahydrated magnesium and cobalt hexammine) may not be identical.

Although cobalt(III) hexammine inhibits catalysis of pre-tRNA cleavage by RNase P in the presence of magnesium, it enhances the catalytic activity of the holoenzyme in the presence of a variety of mainly softer divalent cations such as cadmium, cobalt, and zinc. A previous measurement (*41*) demonstrated activation of *E. coli* P RNA-catalyzed pre-tRNA cleavage by Zn^{2+} in the presence of Sr^{2+}, Ba^{2+}, or $Co(NH_3)_6^{3+}$, but at a sharply reduced rate (60-fold less) compared to pre-tRNA cleavage in the presence of Mg^{2+}. However, the high activity of the Zn^{2+}-activated holoenzyme [within 5-fold of magnesium(II)-activated catalysis] is unprecedented. Moreover, this is the first time that significant activation of RNase P activity by Co^{2+} has been demonstrated. This enhancement likely reflects the ability of $Co(NH_3)_6^{3+}$ both to stabilize nativelike P RNA structure (*76*) and to compete with inhibitory Cd^{2+}, Co^{2+}, or Zn^{2+} ions. The transition metals, Mn^{2+} and Zn^{2+}, are better Lewis acids than magnesium, and therefore compete with $Co(NH_3)_6^{3+}$ to activate RNase P at concentrations ≥30-fold lower than Mg^{2+} (Figure 8; K_{app} = 0.3−0.6 mM versus >20 mM for Mg^{2+}). Unlike magnesium ions, however, these metal ions favor inner-sphere contacts with the imino nitrogens of the nucleic acid bases in addition to phosphate oxygens (*85*), which may lead to the formation of inhibitory metal sites. This difference in coordination preference likely explains the inability of softer ions to completely substitute for magnesium in folding and/or catalysis. The activation of RNase P catalysis by a variety of divalent transition metal ions, but not cobalt hexammine, suggests (but does not prove) that at least one metal ion plays an essential functional role that requires the ionization or the displacement of H_2O from the metal hydration shell (*26*). Such functional roles include: (i) direct coordination of the 3′-oxyanion leaving group of the 5′-leader (*67*); (ii) direct coordination of nonbridging phos-

phate oxygens at the cleavage site (*63*−*66*); or (iii) stabilization of a nucleophilic hydroxide ion (*17*, *25*).

Conclusions. The protein component plays an important role in decreasing the magnesium ion dependence of RNase P catalysis. This is *not* achieved by altering the number or function of magnesium ions involved in stabilizing the global P RNA fold or tRNA binding. However, the protein component does increase the apparent affinities of specific magnesium ions that stabilize pre-tRNA binding and, perhaps, cleavage. A Hill coefficient of 4 suggests that at least 4 magnesium ion binding sites, or classes of sites, stabilize the RNase P·pre-tRNA complex.

These results do not indicate that the protein alters magnesium binding affinity by a direct interaction with these metals (either by coordination or by hydrogen bonding). Rather, this increase in magnesium ion affinity is coupled to the role of the protein in stabilizing pre-tRNA binding to RNase P through contacts with the 5′-leader sequence. Furthermore, the protein component does not appear to play a significant role in directly stabilizing the transition state or the ionization of crucial active site moieties. Cobalt(III) hexammine inhibition of pre-tRNA cleavage and the sensitivity of catalysis to metal ion identity are consistent with a catalytic role for one or more metal ions in RNase P.

ACKNOWLEDGMENT

Dr. Sharon M. Crary provided purified T4 DNA ligase for use in RNA ligation reactions. We thank Dr. Crary, Dr. S. Niranjanakumari, Jeremy Day, and Andy Andrews for helpful discussions.

REFERENCES

1. Pace, N. R., and Brown, J. W. (1995) *J. Bacteriol. 177*, 1919−1928.
2. Frank, D. N., and Pace, N. R. (1998) *Annu. Rev. Biochem. 67*, 153−180.
3. Schön, A. (1999) *FEMS Microbiol. Rev. 23*, 391−406.
4. Schedl, P., and Primakoff, P. (1973) *Proc. Natl. Acad. Sci. U.S.A. 70*, 2091−2095.
5. Stark, B. C., Kole, R., Bowman, E. J., and Altman, S. (1978) *Proc. Natl. Acad. Sci. U.S.A. 75*, 3717−3721.
6. Gardiner, K., and Pace, N. R. (1980) *J. Biol. Chem. 255*, 7507−7509.
7. Baer, M. F., Wesolowski, D., and Altman, S. (1989) *J. Bacteriol. 171*, 6862−6866.
8. Guerrier-Takada, C., Gardiner, K., Marsh, T., Pace, N., and Altman, S. (1983) *Cell 35*, 849−857.
9. Gardiner, K. J., Marsh, T. L., and Pace, N. R. (1985) *J. Biol. Chem. 260*, 5415−5419.
10. Reich, C., Olsen, G. J., Pace, B., and Pace, N. R. (1988) *Science 239*, 178−181.
11. Cowan, J. A. (1995) in *The Biological Chemistry of Magnesium* (Cowan, J. A., Ed.) pp 1−23, VCH Publishers, Inc., New York.
12. Cowan, J. A. (1997) *J. Biol. Inorg. Chem. 2*, 168−176.
13. Beebe, J. A., Kurz, J. C., and Fierke, C. A. (1996) *Biochemistry 35*, 10493−10505.
14. Misra, V. K., and Draper, D. E. (1998) *Biopolymers 48*, 113−135.
15. Pan, T. (1995) *Biochemistry 34*, 902−909.
16. Loria, A., Niranjanakumari, S., Fierke, C. A., and Pan, T. (1998) *Biochemistry 37*, 15466−15473.
17. Smith, D., and Pace, N. R. (1993) *Biochemistry 32*, 5273−5281.
18. Caprara, M. G., Myers, C. A., and Lambowitz, A. M. (2001) *J. Mol. Biol. 308*, 165−190.
19. Gerstner, R. B., Pak, Y., and Draper, D. E. (2001) *Biochemistry 40*, 7165−7173.
20. Crary, S. M., Niranjanakumari, S., and Fierke, C. A. (1998) *Biochemistry 37*, 9409−9416.
21. Kurz, J. C., Niranjanakumari, S., and Fierke, C. A. (1998) *Biochemistry 37*, 2393−2400.
22. Niranjanakumari, S., Stams, T., Crary, S. M., Christianson, D. W., and Fierke, C. A. (1998) *Proc. Natl. Acad. Sci. U.S.A. 95*, 15212−15217.
23. Stams, T., Niranjanakumari, S., Fierke, C. A., and Christianson, D. W. (1998) *Science 280*, 752−755.
24. Fersht, A. (1985) *Enzyme Structure and Mechanism*, 2nd ed., W. H. Freeman and Co., New York.
25. Pyle, A. M. (1993) *Science 261*, 709−714.
26. Cowan, J. A. (1993) *J. Inorg. Biochem. 49*, 171−175.
27. Milligan, J. F., and Uhlenbeck, O. C. (1989) *Methods Enzymol. 180*, 51−62.
28. Beebe, J. A., and Fierke, C. A. (1994) *Biochemistry 33*, 10294−10304.
29. Studier, F. W., Rosenberg, A. H., Dunn, J. J., and Dubendorff, J. W. (1990) *Methods Enzymol. 185*, 60−89.
30. Niranjanakumari, S., Kurz, J. C., and Fierke, C. A. (1998) *Nucleic Acids Res. 26*, 3090−3096.
31. Moore, M. J., and Sharp, P. A. (1992) *Science 256*, 992−997.
32. Ellis, K. J., and Morrison, J. F. (1982) *Methods Enzymol. 87*, 405−426.
33. Bell, J. E., and Bell, E. T. (1988) *Proteins and Enzymes*, Prentice-Hall, Englewood Cliffs, NJ.
34. Fierke, C. A., and Hammes, G. G. (1995) *Methods Enzymol. 249*, 3−37.
35. Cantor, C. R., and Schimmel, P. R. (1980) *The Behavior of Macromolecules*, Vol. III, W. H. Freeman and Co., New York.
36. Feig, A. L., and Uhlenbeck, O. C. (1999) in *The RNA World* (Gesteland, R. F., Cech, T. R., and Atkins, J. F., Eds.) pp 287−319, Cold Spring Harbor Laboratory Press, Cold Spring Harbor, NY.
37. Oh, B. K., Frank, D. N., and Pace, N. R. (1998) *Biochemistry 37*, 7277−7283.
38. Biswas, R., Ledman, D. W., Fox, R. O., Altman, S., and Gopalan, V. (2000) *J. Mol. Biol. 296*, 19−31.
39. Sharkady, S. M., and Nolan, J. M. (2001) *Nucleic Acids Res. 29*, 3848−3856.
40. Cech, T. R., and Bass, B. L. (1986) *Annu. Rev. Biochem. 55*, 599−629.
41. Brännvall, M., and Kirsebom, L. A. (2001) *Proc. Natl. Acad. Sci. U.S.A. 98*, 12943−12947.
42. Juneau, K., Podell, E., Harrington, D. J., and Cech, T. (2001) *Structure 9*, 221−231.
43. Suga, H., Cowan, J. A., and Szostak, J. W. (1998) *Biochemistry 37*, 10118−10125.
44. Nesbitt, S., Hegg, L. A., and Fedor, M. J. (1997) *Chem. Biol. 4*, 619−630.
45. Nakano, S., Chadalavada, D. M., and Bevilacqua, P. C. (2000) *Science 287*, 1493−1497.
46. Smith, D., Burgin, A. B., Haas, E. S., and Pace, N. R. (1992) *J. Biol. Chem. 267*, 2429−2436.
47. Surratt, C. K., Carter, B. J., Payne, R. C., and Hecht, S. M. (1990) *J. Biol. Chem. 265*, 22513−22519.
48. Guerrier-Takada, C., Haydock, K., Allen, L., and Altman, S. (1986) *Biochemistry 25*, 1509−1515.
49. Pannucci, J. A., Haas, E. S., Hall, T. A., Harris, J. K., and Brown, J. W. (1999) *Proc. Natl. Acad. Sci. U.S.A. 96*, 7803−7808.
50. Rialdi, G., Levy, J., and Biltonen, R. (1972) *Biochemistry 11*, 2472−2479.
51. Römer, R., and Hach, R. (1975) *Eur. J. Biochem. 55*, 271−284.
52. Bina-Stein, M., and Stein, A. (1976) *Biochemistry 15*, 3912−3917.
53. Stein, A., and Crothers, D. M. (1976) *Biochemistry 15*, 157−160.
54. Manning, G. S. (1978) *Q. Rev. Biophys. 11*, 179−246.
55. Anderson, C. F., and Record, M. T., Jr. (1990) *Annu. Rev. Biophys. Biophys. Chem. 19*, 423−465.
56. Anderson, C. F., and Record, M. T., Jr. (1995) *Annu. Rev. Phys. Chem. 46*, 657−700.
57. Manning, G. S., and Ray, J. (1998) *J. Biomol. Struct. Dyn. 16*, 461−476.
58. Pan, T., and Sosnick, T. R. (1997) *Nat. Struct. Biol. 4*, 931−938.
59. Fang, X., Pan, T., and Sosnick, T. R. (1999) *Biochemistry 38*, 16840−16846.
60. Fang, X. W., Pan, T., and Sosnick, T. R. (1999) *Nat. Struct. Biol. 6*, 1091−1095.
61. Fang, X., Littrell, K., Yang, X. J., Henderson, S. J., Siefert, S., Thiyagarajan, P., Pan, T., and Sosnick, T. R. (2000) *Biochemistry 39*, 11107−11113.

62. Fang, X. W., Yang, X. J., Littrell, K., Niranjanakumari, S., Thiyagarajan, P., Fierke, C. A., Sosnick, T. R., and Pan, T. (2001) *RNA 7*, 233−241.
63. Chen, Y., Li, X., and Gegenheimer, P. (1997) *Biochemistry 36*, 2425−2438.
64. Warnecke, J. M., Fürste, J. P., Hardt, W. D., Erdmann, V. A., and Hartmann, R. K. (1996) *Proc. Natl. Acad. Sci. U.S.A. 93*, 8924−8928.
65. Warnecke, J. M., Held, R., Busch, S., and Hartmann, R. K. (1999) *J. Mol. Biol. 290*, 433−445.
66. Warnecke, J. M., Green, C. J., and Hartmann, R. K. (1997) *Nucleosides Nucleotides 16*, 721−725.
67. Warnecke, J. M., Sontheimer, E. J., Piccirilli, J. A., and Hartmann, R. K. (2000) *Nucleic Acids Res. 28*, 720−727.
68. Conrad, F., Hanne, A., Gaur, R. K., and Krupp, G. (1995) *Nucleic Acids Res. 23*, 1845−1853.
69. Gaur, R. K., and Krupp, G. (1993) *Nucleic Acids Res. 21*, 21−26.
70. Hardt, W. D., Warnecke, J. M., Erdmann, V. A., and Hartmann, R. K. (1995) *EMBO J. 14*, 2935−2944.
71. Harris, M. E., and Pace, N. R. (1995) *RNA 1*, 210−218.
72. Kazantsev, A. V., and Pace, N. R. (1998) *RNA 4*, 937−947.
73. Christian, E. L., Kaye, N. M., and Harris, M. E. (2000) *RNA 6*, 511−519.
74. Crary, S. M., Kurz, J. C., and Fierke, C. A. (2002) *RNA* (in press).
75. Loria, A., and Pan, T. (1999) *Biochemistry 38*, 8612−8620.
76. Brännvall, M., Mikkelsen, N. E., and Kirsebom, L. A. (2001) *Nucleic Acids Res. 29*, 1426−1432.
77. Pearson, R. G. (1988) *Inorg. Chem. 27*, 734−740.
78. Kazakov, S., and Altman, S. (1991) *Proc. Natl. Acad. Sci. U.S.A. 88*, 9193−9197.
79. Black, C. B., and Cowan, J. A. (1994) *J. Am. Chem. Soc. 116*, 1174−1178.
80. Colmenarejo, G., and Tinoco, I., Jr. (1999) *J. Mol. Biol. 290*, 119−135.
81. Gonzalez, R. L., Jr., and Tinoco, I., Jr. (1999) *J. Mol. Biol. 289*, 1267−1282.
82. Maderia, M., Horton, T. E., and DeRose, V. J. (2000) *Biochemistry 39*, 8193−8200.
83. Rüdisser, S., and Tinoco, I., Jr. (2000) *J. Mol. Biol. 295*, 1211−1223.
84. Schmitz, M., and Tinoco, I., Jr. (2000) *RNA 6*, 1212−1225.
85. Sigel, H. (1993) *Chem. Soc. Rev. 22*, 255−267.

BI025553W